Figure S1

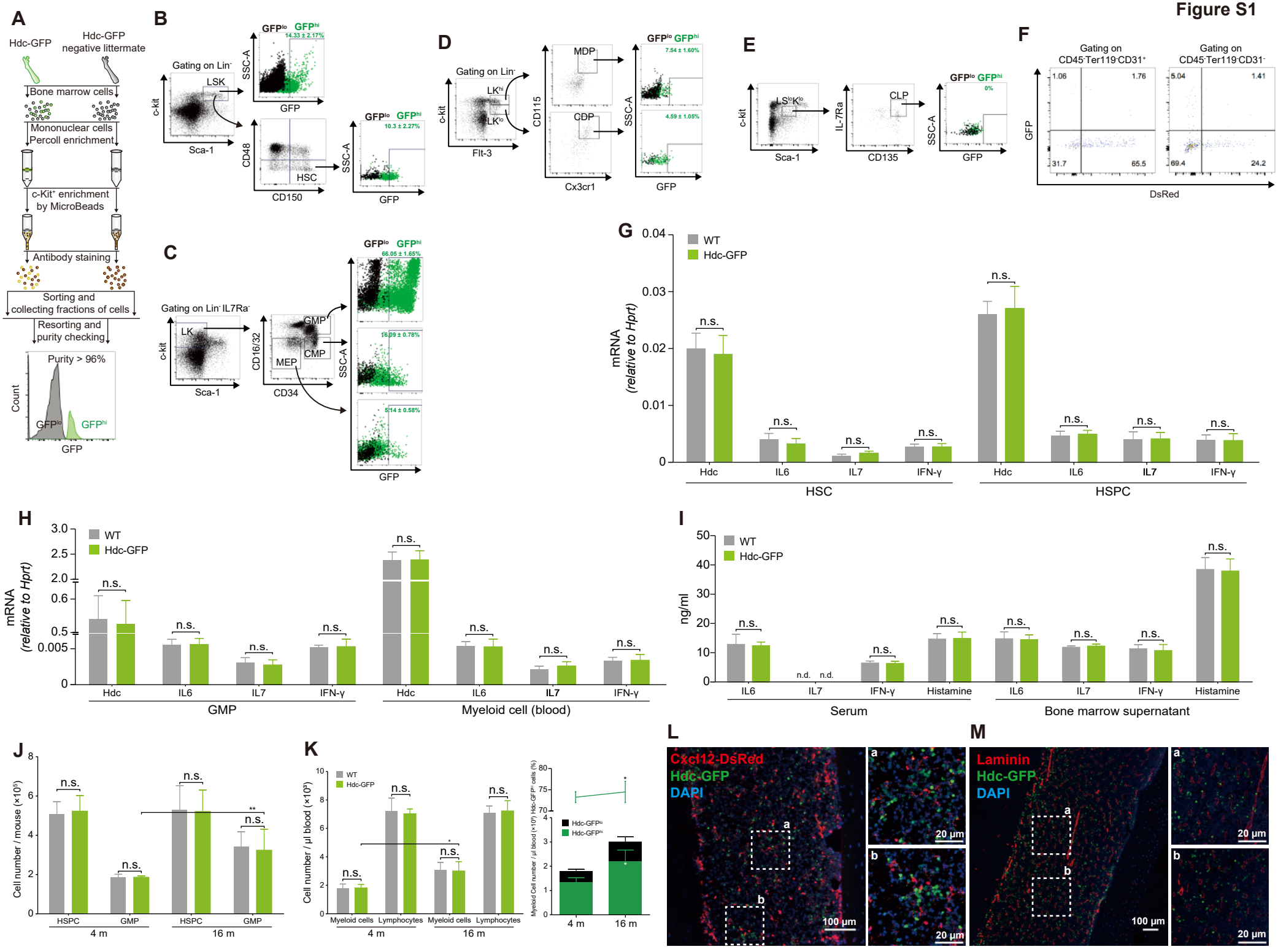
A
Hdc-GFP
Hdc-GFP negative littermate
Bone marrow cells
Mononuclear cells Percoll enrichment
c-Kit+ enrichment by MicroBeads
Antibody staining
Sorting and collecting fractions of cells
Resorting and purity checking
Purity > 96%
Count
GFP
B
Gating on Lin-
LSK
SSC-A
GFP
c-kit
Sca-1
CD48
HSC
CD150
C
Gating on Lin- IL7Ra-
LK
GMP
MEP
CMP
CD16/32
CD34
D
Gating on Lin-
LKhi
LKlo
Flt-3
MDP
CDP
CD115
Cx3cr1
E
LSloklo
CLP
IL-7Ra
CD135
F
Gating on CD45-Ter119-CD31+
Gating on CD45-Ter119-CD31-
DsRed
G
WT
Hdc-GFP
mRNA (relative to Hprt)
n.s.
Hdc
IL6
IL7
IFN-γ
HSC
HSPC
H
GMP
Myeloid cell (blood)
I
ng/ml
n.d.
Serum
Bone marrow supernatant
Histamine
J
Cell number / mouse (×10⁵)
HSPC
GMP
4 m
16 m
K
Cell number / μl blood (×10³)
Myeloid cells
Lymphocytes
Hdc-GFPlo
Hdc-GFPhi
L
Cxcl12-DsRed
Hdc-GFP
DAPI
100 μm
20 μm
M
Laminin
Hdc-GFP
DAPI

Figure S2

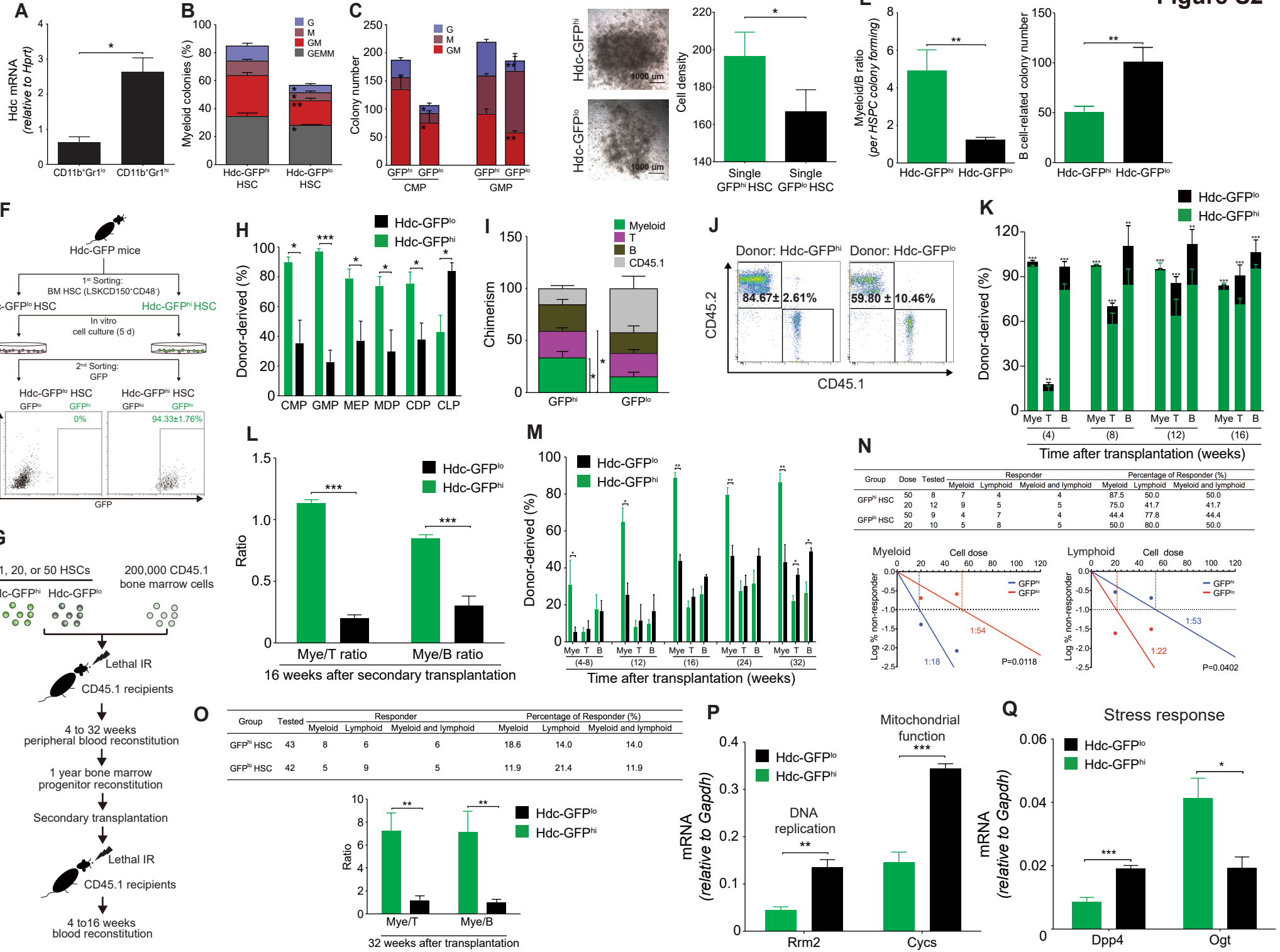

Group	Dose	Tested	Responder			Percentage of Responder (%)		
			Myeloid	Lymphoid	Myeloid and lymphoid	Myeloid	Lymphoid	Myeloid and lymphoid
GFP^{hi} HSC	50	8	7	4	4	87.5	50.0	50.0
	20	12	9	5	5	75.0	41.7	41.7
GFP^{lo} HSC	50	9	4	7	4	44.4	77.8	44.4
	20	10	5	8	5	50.0	80.0	50.0

Group	Tested	Responder			Percentage of Responder (%)		
		Myeloid	Lymphoid	Myeloid and lymphoid	Myeloid	Lymphoid	Myeloid and lymphoid
GFP^{hi} HSC	43	8	6	6	18.6	14.0	14.0
GFP^{lo} HSC	42	5	9	5	11.9	21.4	11.9

Figure S3

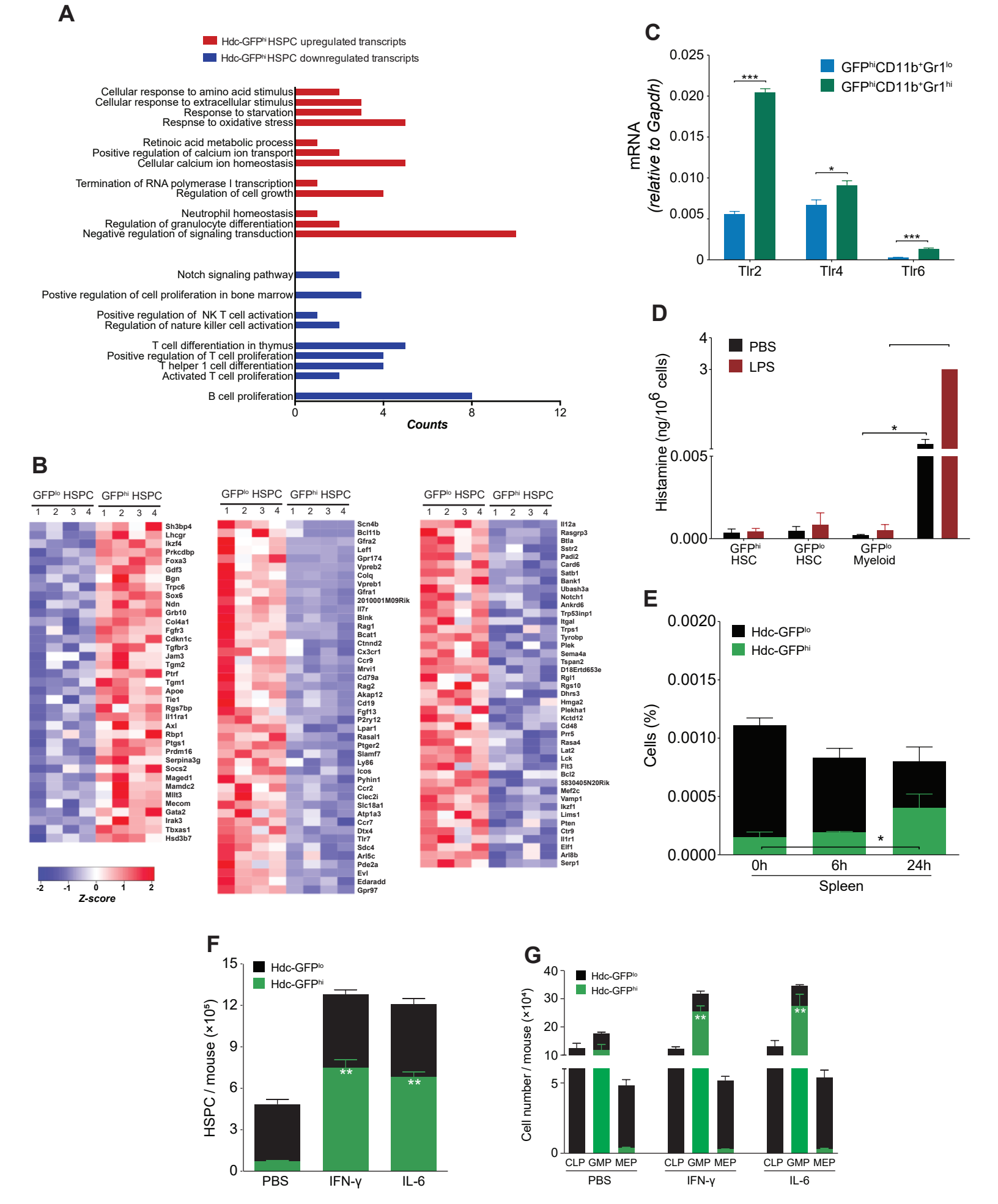
A
Hdc-GFPhi HSPC upregulated transcripts
Hdc-GFPhi HSPC downregulated transcripts
Cellular response to amino acid stimulus
Cellular response to extracellular stimulus
Response to starvation
Respnse to oxidative stress
Retinoic acid metabolic process
Positive regulation of calcium ion transport
Cellular calcium ion homeostasis
Termination of RNA polymerase I transcription
Regulation of cell growth
Neutrophil homeostasis
Regulation of granulocyte differentiation
Negative regulation of signaling transduction
Notch signaling pathway
Postive regulation of cell proliferation in bone marrow
Positive regulation of NK T cell activation
Regulation of nature killer cell activation
T cell differentiation in thymus
Positive regulation of T cell proliferation
T helper 1 cell differentiation
Activated T cell proliferation
B cell proliferation
0
4
8
12
Counts
B
GFPlo HSPC
GFPhi HSPC
1 2 3 4
Sh3bp4
Lhcgr
Ikzf4
Prkcdbp
Foxa3
Gdf3
Bgn
Trpc6
Sox6
Ndn
Grb10
Col4a1
Fgfr3
Cdkn1c
Tgfbr3
Jam3
Tgm2
Ptrf
Tgm1
Apoe
Tie1
Rgs7bp
Il11ra1
Axl
Rbp1
Ptgs1
Prdm16
Serpina3g
Socs2
Maged1
Mamdc2
Mllt3
Mecom
Gata2
Irak3
Tbxas1
Hsd3b7
Scn4b
Bcl11b
Gfra2
Lef1
Gpr174
Vpreb2
Colq
Vpreb1
Gfra1
2010001M09Rik
Il7r
Blnk
Rag1
Bcat1
Ctnnd2
Cx3cr1
Ccr9
Mrvi1
Cd79a
Rag2
Akap12
Cd19
Fgf13
P2ry12
Lpar1
Rasal1
Ptger2
Slamf7
Ly86
Icos
Pyhin1
Ccr2
Clec2i
Slc18a1
Atp1a3
Ccr7
Dtx4
Tlr7
Sdc4
Arl5c
Pde2a
Evl
Edaradd
Gpr97
Il12a
Rasgrp3
Btla
Sstr2
Padi2
Card6
Satb1
Bank1
Ubash3a
Notch1
Ankrd6
Trp53inp1
Itgal
Trps1
Tyrobp
Plek
Sema4a
Tspan2
D18Ertd653e
Rgl1
Rgs10
Dhrs3
Hmga2
Plekha1
Kctd12
Cd48
Prr5
Rasa4
Lat2
Lck
Flt3
Bcl2
5830405N20Rik
Mef2c
Vamp1
Ikzf1
Lims1
Pten
Ctr9
Il1r1
Elf1
Arl8b
Serp1
-2 -1 0 1 2
Z-score
C
mRNA (relative to Gapdh)
0.025
0.020
0.015
0.010
0.005
0
GFPhiCD11b+Gr1lo
GFPhiCD11b+Gr1hi
***
*
***
Tlr2
Tlr4
Tlr6
D
Histamine (ng/10^6 cells)
4
3
0.005
0.000
PBS
LPS
*
GFPhi HSC
GFPlo HSC
GFPlo Myeloid
E
Cells (%)
0.0020
0.0015
0.0010
0.0005
0.0000
Hdc-GFPlo
Hdc-GFPhi
*
0h
6h
24h
Spleen
F
HSPC / mouse (×10^5)
15
12
9
6
3
0
Hdc-GFPlo
Hdc-GFPhi
**
**
PBS
IFN-γ
IL-6
G
Cell number / mouse (×10^4)
40
30
20
10
5
0
Hdc-GFPlo
Hdc-GFPhi
**
**
CLP GMP MEP
PBS
CLP GMP MEP
IFN-γ
CLP GMP MEP
IL-6

Figure S4

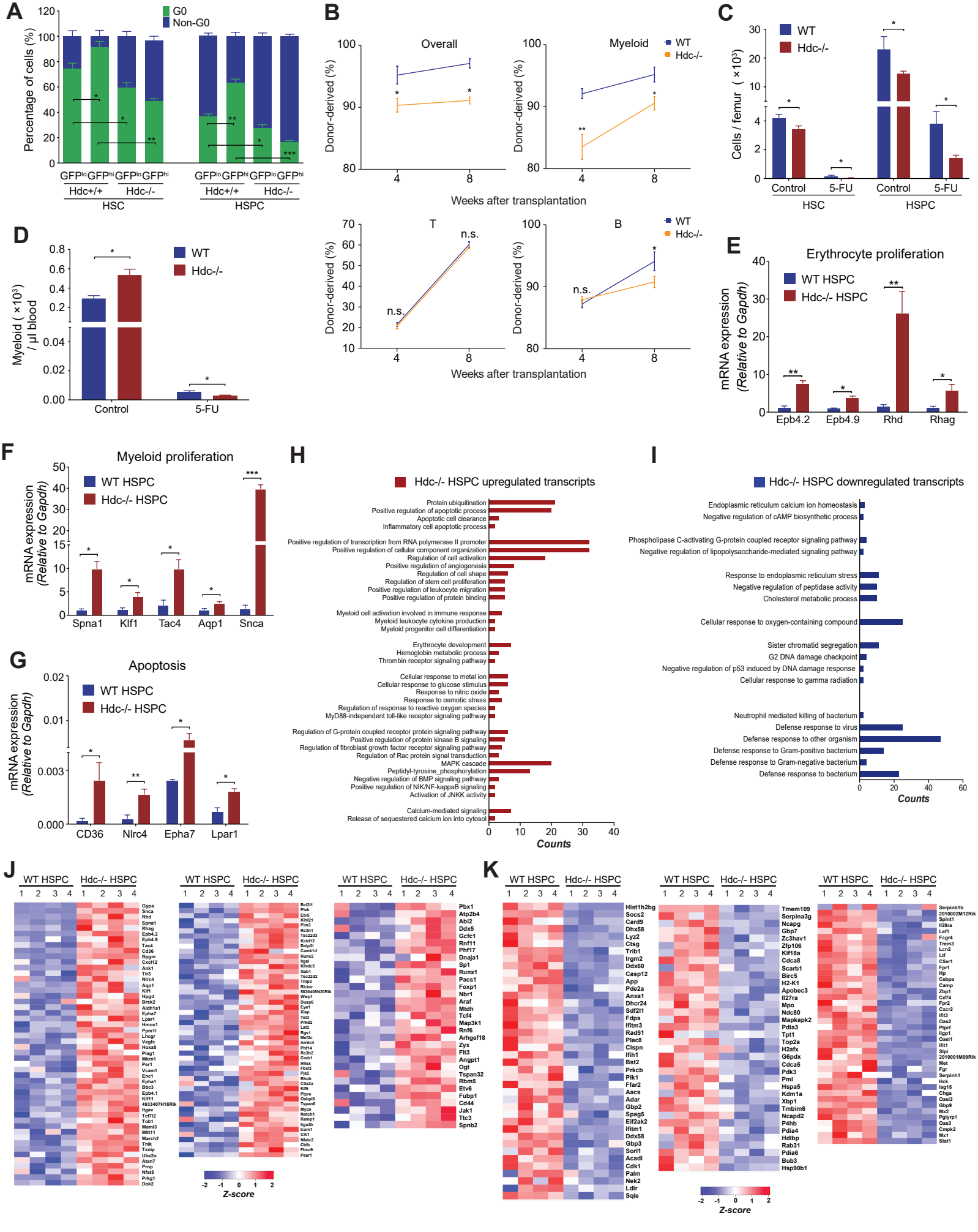
A
G0
Non-G0
Percentage of cells (%)
GFPloGFPhi GFPloGFPhi GFPloGFPhi GFPloGFPhi
Hdc+/+ Hdc-/- Hdc+/+ Hdc-/-
HSC
HSPC
B
Overall
Myeloid
WT
Hdc-/-
Donor-derived (%)
Weeks after transplantation
T
B
n.s.
C
Cells / femur (×10³)
Control
5-FU
HSC
HSPC
D
Myeloid (×10³) / µl blood
E
Erythrocyte proliferation
WT HSPC
Hdc-/- HSPC
mRNA expression (Relative to Gapdh)
Epb4.2
Epb4.9
Rhd
Rhag
F
Myeloid proliferation
Spna1
Klf1
Tac4
Aqp1
Snca
G
Apoptosis
CD36
Nlrc4
Epha7
Lpar1
H
Hdc-/- HSPC upregulated transcripts
Protein ubiquitination
Positive regulation of apoptotic process
Apoptotic cell clearance
Inflammatory cell apoptotic process
Positive regulation of transcription from RNA polymerase II promoter
Positive regulation of cellular component organization
Regulation of cell activation
Positive regulation of angiogenesis
Regulation of cell shape
Regulation of stem cell proliferation
Positive regulation of leukocyte migration
Positive regulation of protein binding
Myeloid cell activation involved in immune response
Myeloid leukocyte cytokine production
Myeloid progenitor cell differentiation
Erythrocyte development
Hemoglobin metabolic process
Thrombin receptor signaling pathway
Cellular response to metal ion
Cellular response to glucose stimulus
Response to nitric oxide
Response to osmotic stress
Regulation of response to reactive oxygen species
MyD88-independent toll-like receptor signaling pathway
Regulation of G-protein coupled receptor protein signaling pathway
Positive regulation of protein kinase B signaling
Regulation of fibroblast growth factor receptor signaling pathway
Regulation of Rac protein signal transduction
MAPK cascade
Peptidyl-tyrosine_phosphorylation
Negative regulation of BMP signaling pathway
Positive regulation of NIK/NF-kappaB signaling
Activation of JNKK activity
Calcium-mediated signaling
Release of sequestered calcium ion into cytosol
Counts
I
Hdc-/- HSPC downregulated transcripts
Endoplasmic reticulum calcium ion homeostasis
Negative regulation of cAMP biosynthetic process
Phospholipase C-activating G-protein coupled receptor signaling pathway
Negative regulation of lipopolysaccharide-mediated signaling pathway
Response to endoplasmic reticulum stress
Negative regulation of peptidase activity
Cholesterol metabolic process
Cellular response to oxygen-containing compound
Sister chromatid segregation
G2 DNA damage checkpoint
Negative regulation of p53 induced by DNA damage response
Cellular response to gamma radiation
Neutrophil mediated killing of bacterium
Defense response to virus
Defense response to other organism
Defense response to Gram-positive bacterium
Defense response to Gram-negative bacterium
Defense response to bacterium
Counts
J
WT HSPC
Hdc-/- HSPC
Z-score
K
Z-score

Figure S5

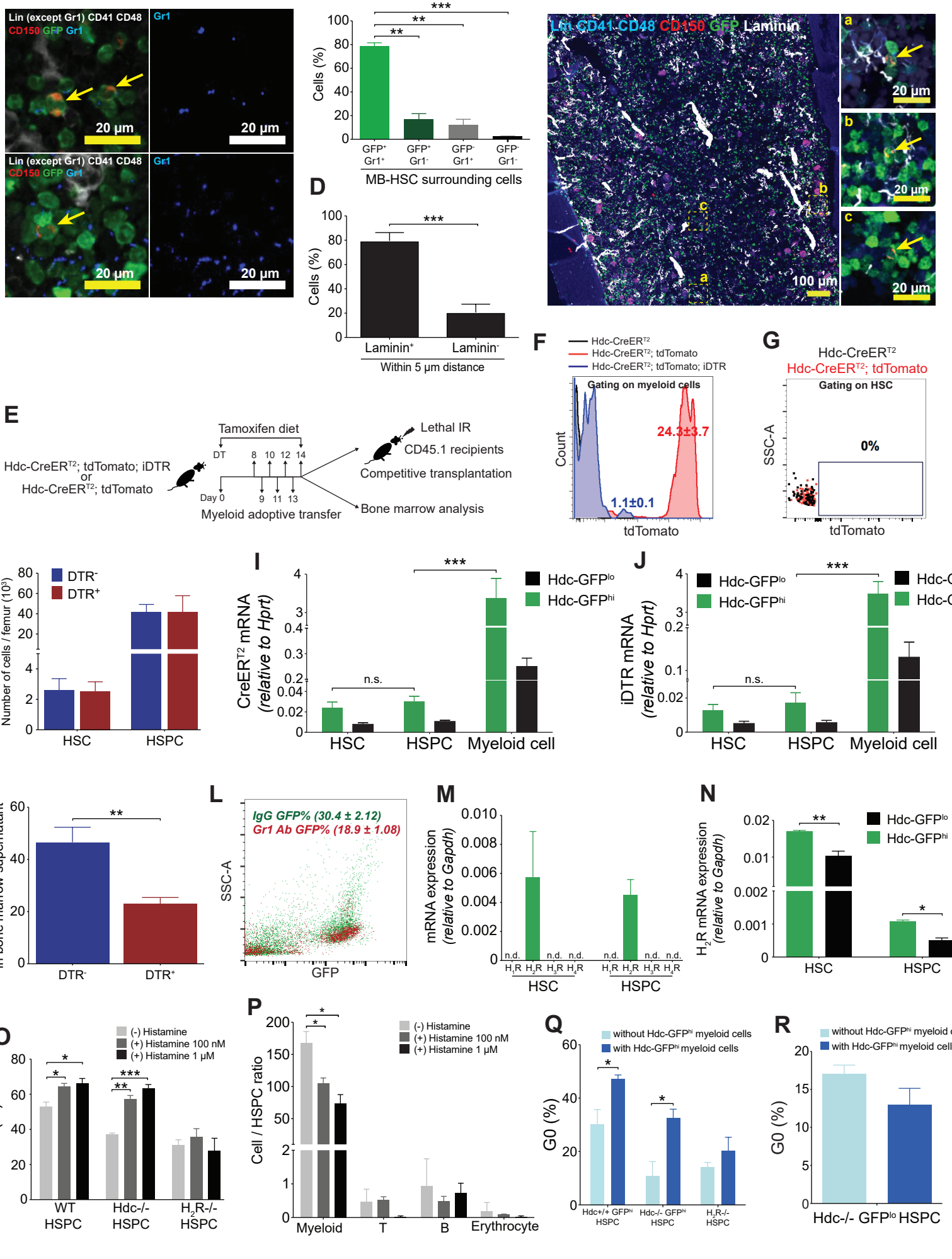
A
Lin (except Gr1) CD41 CD48
CD150 GFP Gr1
Gr1
20 μm
B
Cells (%)
GFP+ Gr1+
GFP+ Gr1-
GFP- Gr1+
GFP- Gr1-
MB-HSC surrounding cells
C
Lin CD41 CD48 CD150 GFP Laminin
100 μm
D
Cells (%)
Laminin+
Laminin-
Within 5 μm distance
E
Tamoxifen diet
DT
Day 0
Hdc-CreER^{T2}; tdTomato; iDTR
or
Hdc-CreER^{T2}; tdTomato
Myeloid adoptive transfer
Lethal IR
CD45.1 recipients
Competitive transplantation
Bone marrow analysis
F
Hdc-CreER^{T2}
Hdc-CreER^{T2}; tdTomato
Hdc-CreER^{T2}; tdTomato; iDTR
Gating on myeloid cells
24.3±3.7
1.1±0.1
Count
tdTomato
G
Hdc-CreER^{T2}
Hdc-CreER^{T2}; tdTomato
Gating on HSC
0%
SSC-A
tdTomato
H
DTR-
DTR+
Number of cells / femur (10^3)
HSC
HSPC
I
CreER^{T2} mRNA (relative to Hprt)
Hdc-GFPlo
Hdc-GFPhi
n.s.
HSC
HSPC
Myeloid cell
J
iDTR mRNA (relative to Hprt)
Hdc-GFPlo
Hdc-GFPhi
n.s.
HSC
HSPC
Myeloid cell
K
Histamine (ng/ml) in bone marrow supernatant
DTR-
DTR+
L
IgG GFP% (30.4 ± 2.12)
Gr1 Ab GFP% (18.9 ± 1.08)
SSC-A
GFP
M
mRNA expression (relative to Gapdh)
n.d.
H1R H2R H3R H4R
HSC
HSPC
N
H2R mRNA expression (relative to Gapdh)
Hdc-GFPlo
Hdc-GFPhi
HSC
HSPC
O
(-) Histamine
(+) Histamine 100 nM
(+) Histamine 1 μM
G0 (%)
WT HSPC
Hdc-/- HSPC
H2R-/- HSPC
P
(-) Histamine
(+) Histamine 100 nM
(+) Histamine 1 μM
Cell / HSPC ratio
Myeloid
T
B
Erythrocyte
Q
without Hdc-GFPhi myeloid cells
with Hdc-GFPhi myeloid cells
G0 (%)
Hdc+/+ GFPhi HSPC
Hdc-/- GFPhi HSPC
H2R-/- HSPC
R
without Hdc-GFPhi myeloid cells
with Hdc-GFPhi myeloid cells
G0 (%)
Hdc-/- GFPlo HSPC

Figure S6

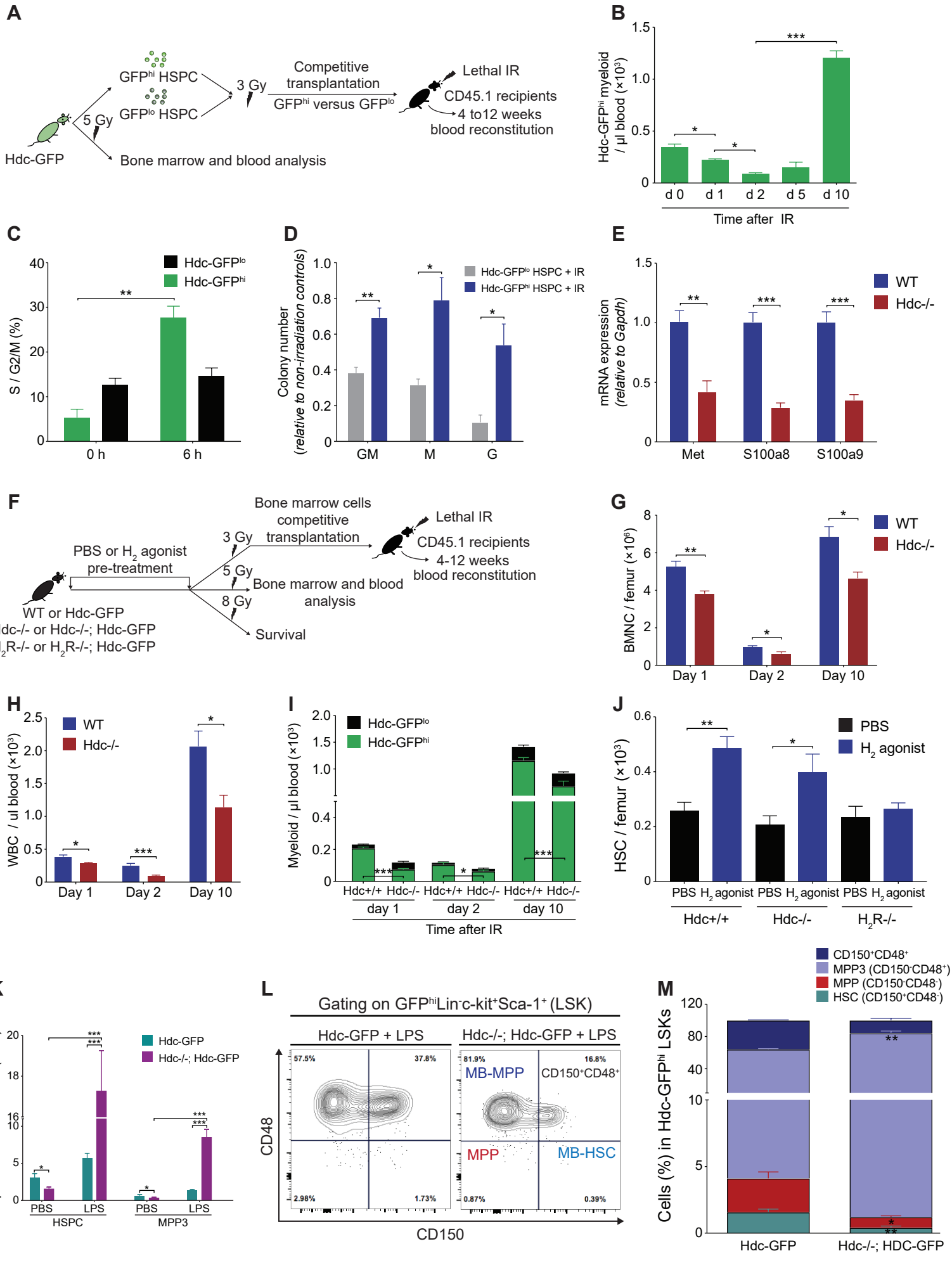
A
GFPhi HSPC
GFPlo HSPC
3 Gy
Competitive transplantation
GFPhi versus GFPlo
Lethal IR
CD45.1 recipients
4 to12 weeks blood reconstitution
5 Gy
Hdc-GFP
Bone marrow and blood analysis
B
Hdc-GFPhi myeloid / µl blood (×10³)
Time after IR
d 0
d 1
d 2
d 5
d 10
C
Hdc-GFPlo
Hdc-GFPhi
S / G2/M (%)
0 h
6 h
D
Hdc-GFPlo HSPC + IR
Hdc-GFPhi HSPC + IR
Colony number (relative to non-irradiation controls)
GM
M
G
E
WT
Hdc-/-
mRNA expression (relative to Gapdh)
Met
S100a8
S100a9
F
Bone marrow cells competitive transplantation
3 Gy
Lethal IR
CD45.1 recipients
4-12 weeks blood reconstitution
PBS or H2 agonist pre-treatment
5 Gy
Bone marrow and blood analysis
8 Gy
Survival
WT or Hdc-GFP
Hdc-/- or Hdc-/-; Hdc-GFP
H2R-/- or H2R-/-; Hdc-GFP
G
BMNC / femur (×10⁶)
Day 1
Day 2
Day 10
H
WBC / ul blood (×10³)
I
Myeloid / µl blood (×10³)
Hdc+/+
Hdc-/-
day 1
day 2
day 10
Time after IR
J
PBS
H2 agonist
HSC / femur (×10³)
Hdc+/+
Hdc-/-
H2R-/-
K
Hdc-GFP
Hdc-/-; Hdc-GFP
Spleen Hdc-GFPhi cells (×10²)
PBS
LPS
HSPC
MPP3
L
Gating on GFPhiLin-c-kit+Sca-1+ (LSK)
Hdc-GFP + LPS
Hdc-/-; Hdc-GFP + LPS
57.5%
37.8%
2.98%
1.73%
81.9%
16.8%
0.87%
0.39%
MB-MPP
CD150+CD48+
MPP
MB-HSC
CD48
CD150
M
CD150+CD48+
MPP3 (CD150-CD48+)
MPP (CD150-CD48-)
HSC (CD150+CD48-)
Cells (%) in Hdc-GFPhi LSKs
Hdc-GFP
Hdc-/-; HDC-GFP

Figure S1. Hdc-GFP Expression in HSCs, Progenitors and BM Stromal Cells, Related to Figure 1

(A) Schematic diagram showing the protocol for HSC cell sorting and assessment of purity. (B-E) Representative flow plots of HSPC ($Lin^-c\text{-}kit^+Sca\text{-}1^+$, LSK) and HSC ($Lin^-c\text{-}kit^+Sca\text{-}1^+CD150^+CD48^-$) (B); $Lin^-IL\text{-}7Ra^-c\text{-}kit^+Sca\text{-}1^-CD34^+CD16/32^{lo}$ common myeloid progenitor (CMP), $Lin^-IL\text{-}7Ra^-c\text{-}kit^+Sca\text{-}1^-CD34^+CD16/32^{hi}$ granulocyte and macrophage progenitor (GMP), and $Lin^-IL\text{-}7Ra^-c\text{-}kit^+Sca\text{-}1^-CD34^-CD16/32^{lo}$ megakaryocyte and erythrocyte progenitor (MEP) (C); $Lin^-Flt\text{-}3^+c\text{-}kit^{hi}CD115^+CX3CR1^+$ macrophage and dendritic cell progenitor (MDP) and $Lin^-Flt\text{-}3^+c\text{-}kit^{lo}CD115^+Cx3cr1^+$ common dendritic progenitor (CDP) (D); $Lin^-c\text{-}kit^{lo}Sca\text{-}1^{lo}Flt\text{-}3^+IL\text{-}7Ra^+$ common lymphoid progenitor (CLP) (E). (F) Representative flow plots of BM stromal endothelial cells ($CD45^-Ter119^-CD31^+$) and mesenchymal progenitor cells ($CD45^-Ter119^-CD31^-$) in Hdc-GFP; Cxcl12-DsRed mice (n = 3). (G and H) mRNA expression levels of Hdc and inflammatory signaling (IL6, IL7, and IFN-γ) in HSCs, HSPCs, GMPs, and blood myeloid cells from Hdc-GFP mice were similar to WT mice (n = 3 per group). (I) Compared to WT mice, protein levels of histamine, IL6, IL7, and IFN-γ in serum and BM supernatant of Hdc-GFP mice showed no significant changes (n = 3 per group). (J and K) The numbers of HSPCs, GMP, blood myeloid cells, and lymphocytes in young (4-month-old) and aged (16-month-old) wild type or Hdc-GFP mice (n = 3 per group) (J). The percentage of Hdc-GFP^{hi} blood myeloid cells (K). (L and M) Representative florescence images of bone frozen sections of Hdc-GFP; Cxcl12-DsRed mice (n = 3) (L) and Hdc-GFP mice (n = 3) bone sections stained with anti-Laminin antibody (M). For all panels, ± SEM is shown. *p < 0.05; **p < 0.01; ***p < 0.001. n.s., not significant. n.d., not detectable. n indicates biological replicates. For all experiments greater than or equal to two independent experiments were performed unless otherwise indicated. Data were analyzed with two-tailed Student's t-test (G-K).

Figure S2. Hdc-GFP^{hi} HSCs and Lineage-committed Progenitors Exhibit Greater Myeloid Lineage Expansion Capacity, Related to Figure 1

(A) $Gr1^{hi}$ cells expressed higher Hdc mRNA within $CD11b^{+}Gr1^{+}$ myeloid population (n = 3 per group). (B) Percentage of myeloid CFU colonies derived from Hdc-GFP^{hi} and Hdc-GFP^{lo} HSCs in M3434 Methylcellulose medium (n = 3 - 5 per group). (C) Myeloid CFU in M3534 Methylcellulose medium, showing numbers of large colonies from CMPs (3,000 Hdc-GFP^{hi} versus Hdc-GFP^{lo}) (n = 4 per group) and GMPs (5,000 Hdc-GFP^{hi} versus Hdc-GFP^{lo}) (n = 3 per group). Five independent experiments. (D) Representative microscopic images (left) and quantification of density (right) of a single colony (25 colonies) grown from sorted single Hdc-GFP^{hi} or Hdc-GFP^{lo} HSC. Five independent experiments. (E) Myeloid/B ratio and B cell-related colony number of colony-forming comparing per Hdc-GFP^{hi} and Hdc-GFP^{lo} HSPCs (n = 4 Hdc-GFP^{hi}, n = 3 Hdc-GFP^{lo}). (F) In vitro culture of Hdc-GFP^{hi} and Hdc-GFP^{lo} HSCs from Hdc-GFP mice, showing the stability (n = 4). (G) Experimental protocol of competitive BM transplantation assays comparing Hdc-GFP^{hi} and Hdc-GFP^{lo} HSCs. (H-J) One year after transplantation, recipient mice of 20 Hdc-GFP^{hi} (n = 6) or Hdc-GFP^{lo} HSCs (n = 5) were analyzed, bar graphs show quantification BM donor-derived progenitors (H) and blood donor chimerism (I). Flow plots (J) show the representative gating of blood donor reconstitution. (K) Donor chimerism in the blood of the secondary recipients from 20 Hdc-GFP^{hi} or Hdc-GFP^{lo} HSCs (n = 10 per recipient group). (L) Blood donor-derived myeloid/B and myeloid/T ratio in secondary BM transplant recipients analyzed in (K) at 16 weeks of secondary transplantation. (M) Contribution of 50 Hdc-GFP^{hi} (n = 8) or Hdc-GFP^{lo} HSCs (n = 9) in the blood of lethally irradiated recipients after transplantation at indicated time points. (N) Limiting dilution assay comparing Hdc-GFP^{hi} or Hdc-GFP^{lo} HSCs, Myeloid or Lymphoid reconstitution potential were examined at 32 weeks after transplantation (n = 8 - 12 per cell dose). Table shows number of responders in each group. (O) Donor Myeloid/T and Myeloid/B reconstitution ratio from recipients transplanted with single Hdc-GFP^{hi} (n = 43) or Hdc-GFP^{lo} HSCs (n = 42) from Hdc-GFP mice. Table shows number of responders in each group. (P and Q) Comparison of mRNA levels of DNA replication and mitochondrial function (P) and stress response genes (Q) between Hdc-GFP^{hi} and Hdc-GFP^{lo} BM HSCs. For all panels, ± SEM is shown. *$p < 0.05$; **$p < 0.01$; ***$p < 0.001$.

n indicates biological replicates. For all experiments greater than or equal to two independent experiments were performed unless otherwise indicated. Data were analyzed with two-tailed Student's t-test (A-C, E-F, H-M, and O-Q), Mann-Whitney test (D), or Poisson distribution with Pearson's chi-squared test (N).

Figure S3. Gene Transcription Profiles and Response to Myeloid or Lymphoid Stimulus Differentially, Related to Figure 1-3

(A) GO biological processes upregulated (red bars) or downregulated (blue bars) in Hdc-GFP^{hi} HSPCs compared to Hdc-GFP^{lo} HSPCs (n = 4 per group). (B) Representative genes based upon GO and KEGG pathways (n = 4 per group). (C) Relative mRNA expression of TLRs in myeloid cell compartments (n = 4 per group). (D) Histamine levels in supernatants from in vitro cultured compartments of HSC or CD11b^{+}Gr1^{+} myeloid cells isolated from Hdc-GFP mice in response to LPS treatment (n = 6 per group). (E) Frequencies of HSCs in spleen of Hdc-GFP mice at 24 hours after LPS treatment (n = 3 - 4 per group). (F-G) Absolute numbers of Hdc-GFP^{hi} and Hdc-GFP^{lo} HSPC (F), CLP, GMP, and MEP (G) in BM of Hdc-GFP mice treated with PBS, IFN-γ, or IL6 (n = 3 per group). For all panels, ± SEM is shown. *p < 0.05; **p < 0.01; ***p < 0.001. n indicates biological replicates. For all experiments greater than or equal to two independent experiments were performed unless otherwise indicated. Data were analyzed with two-tailed Student's t-test (C, D, and F-G) or one-way analysis of variation (ANOVA) with Bonferroni post-hoc test (E).

Figure S4. Increased Myeloid Proliferation in Hdc-/- mice, Related to Figure 4

(A) Cell cycle analyses of BM Hdc-GFP^{hi} and Hdc-GFP^{lo} HSCs and progenitors of Hdc-GFP mice (n = 3) and Hdc-/-; Hdc-GFP mice (n = 4). (B) Noncompetitive transplantation of 4 × 10^{5} unfractionated BM cells from Hdc-/- mice (45.2) or Hdc+/+ age-matched littermates into lethally irradiated WT mice (45.1). Analyses of peripheral blood reconstitution at 4 and 8 weeks (n = 10 per group). (C-D) Mice were intravenously injected with 250 mg/kg 5-FU, and the number of BM HSCs and HSPCs (C) and blood myeloid cells (D) was quantified 5 days after 5-FU treatment (n = 5 per group). (E-G) qRT-PCR analysis shows upregulation of erythrocyte proliferation (E), myeloid proliferation (F), and

apoptosis genes (G) in Hdc-/- HSPCs compared to WT controls (n = 4 per group). (H-K) Biological processes in GO and KEGG pathway analysis that were upregulated (H) or downregulated (I) in Hdc-/- HSPCs compared to WT controls (n = 4 per group); (J) and (K) showing representative genes analyzed in GO and KEGG pathway. For all panels, ± SEM is shown. *p < 0.05; **p < 0.01; ***p < 0.001. n indicates biological replicates. For all experiments greater than or equal to two independent experiments were performed unless otherwise indicated. Data were analyzed with one-way analysis of variation (ANOVA) with Bonferroni post-hoc test (A) or two-tailed Student's t-test (B-G).

Figure S5. Histamine/H_2R Axis Maintains BM HSC Quiescence, Related to Figure 5

(A and B) Direct contact between MB-HSCs and GFP^+Gr1^+ myeloid cells on frozen bone sections, showing representative single MB-HSCs (yellow arrows) surrounded by GFP^+Gr1^+ myeloid cells (left) and quantification (B). Four independent experiments. (C and D) Distribution (C) and quantification (D) of GFP^+ MB-HSC and myeloid clusters in close proximity (< 5 μm) to $Laminin^+$ matrix and vessels on bone frozen sections. Inserts show magnified images demonstrating representative clusters composed of one MB-HSC and two (a) or more than two (b) Hdc-GFP^+ myeloid cells. (c) Magnified image shows a representative cluster that was not close to $Laminin^+$ cells. Four independent experiments. (E) Experimental protocol of Hdc^{hi} myeloid cell depletion and rescue studies. (F) Representative flow histogram showing tdTomato expression in $CD11b^+Gr1^+$ myeloid cells from iDTR/DT experimental groups in Figure 5D. (G) Representative plots showing no expression of tdTomato in HSCs of Hdc-$CreER^{T2}$; tdTomato mice received 2 weeks of tamoxifen diet treatment. (H) Quantification of BM HSCs and HSPCs in tamoxifen/DT-treated Hdc-$CreER^{T2}$; tdTomato; iDTR mice (n = 6 - 8 per group). (I-J) mRNA levels of $CreER^{T2}$ (I) and iDTR (J) in Hdc-GFP^{hi} or Hdc-GFP^{lo} HSC, HSPC, and myeloid cells (n = 4 per group). (K) Histamine levels (ng/ml) measured in the BM cell-free supernatant in groups of DT-treated DTR^+ and DTR^- mice (n = 5 - 6 per group). (L) Representative flow plots of BM Hdc-GFP^{hi} cells in Hdc-GFP mice analyzed in Figure 5F. (M) Analysis of histamine receptor mRNA expression by qRT-PCR in HSCs (n = 4) and HSPCs (n = 3).

(N) Relative expression of H_2R in Hdc-GFP^{hi} or Hdc-GFP^{lo} HSCs or progenitors (n = 3). (O) The frequency of G0 cells in HSPCs in stroma co-culture with or without the addition of histamine (n = 5 - 6 per group). (P) Lineage of cells/HSPCs ratio from the co-culture of Hdc-/- HSPCs with Hdc-/- stromal cells to which was added exogenous H_2 agonist (n = 4 per group) or PBS (n = 4). (Q and R) Quantification of percentage of G0 phase cells in HSPCs in triple cell co-culture system (n = 4 - 6 per group). For all panels, ± SEM is shown. *p < 0.05; **p < 0.01; ***p < 0.001. n.d., not detectable. n indicates biological replicates. For all experiments greater than or equal to two independent experiments were performed unless otherwise indicated. Data were analyzed with one-way analysis of variation (ANOVA) with Bonferroni post-hoc test (B and O), two-tailed Student's t-test (D, H-J, and M, N, and P-R).

Figure S6. H_2 Agonist Protects HSC from Injury, Related to Figure 6

(A) Experimental protocol. (B) Number of Hdc-GFP^{+} myeloid cells in blood of 5 Gy-irradiated Hdc-GFP mice. (C) Frequencies of S/G2/M phase of HSCs showing Hdc-GFP^{hi} and Hdc-GFP^{lo} compartments, respectively, in Hdc-GFP mice BM after 5 Gy of radiation. (D) 3 Gy-irradiated 1500 Hdc-GFP^{hi} HSPCs expanded more myeloid colonies in vitro than the same number of Hdc-GFP^{lo} HSPCs which received the same dosage of IR (n = 3 per group). Data are presented as relative to non-irradiated control. (E) qRT-PCR analysis of stress responsive genes, which were downregulated in Hdc-/- BM HSPCs compared to WT controls (n = 4 per group). (F) Experimental protocol of H_2 agonist on radiation protection experiments. (G and H) BM nucleated cell (BMNC) number (G) and white blood cell (WBC) number (H) in WT or Hdc-/- mice after 5 Gy of radiation. (I) Number of blood myeloid cells in mice after 5 Gy of radiation. (J) Number of HSCs in 5 Gy-irradiated WT, Hdc-/-, or H_2R-/- mice pretreated with either H_2 agonist or PBS (n = 4 - 5 per group). (K) Absolute number of spleen Hdc-GFP^{hi} MB-HSPCs and Hdc-GFP^{hi} MB-MPP (MPP3) in LPS-treated Hdc-GFP (n = 6), Hdc-/-; Hdc-GFP mice (n = 5), and PBS controls (n = 3 - 5 per group) at 24 hours. (L and M) Net frequencies of BM HSCs and multipotent progenitors in LPS treated mice (n = 4 per group), shows representative plots in (H), and quantification in (I). For all panels, ± SEM is shown. *p < 0.05; **p < 0.01; ***p

< 0.001. n indicates biological replicates. For all experiments greater than or equal to two independent experiments were performed unless otherwise indicated. Data were analyzed with one-way analysis of variation (ANOVA) with Bonferroni post-hoc test (B), two-tailed Student’s t-test (C-E, G-K, and M).

Gene Symbol	Organism	Gene Name	Forward Primer (5'- 3')	Reverse Primer (5' - 3')
Nr4a1	Mus musculus	nuclear receptor subfamily 4, group A, member 1	GCCTAGCACTGCCAAATTG	TCTGCCCACTTTCGGATAAC
Cxcr2	Mus musculus	chemokine (C-X-C motif) receptor 2	TCTTCCAGTTCAACCAGCC	ATCCACCTTGAATTCTCCCATC
Mmp9	Mus musculus	matrix metallopeptidase 9	GATCCCCAGAGCGTCATTC	CCACCTTGTTCACCTCATTTTG
Slpi	Mus musculus	secretory leukocyte peptidase inhibitor	GATCCCCAGAGCGTCATTC	CCACCTTGTTCACCTCATTTTG
Ap3b1	Mus musculus	adaptor-related protein complex 3, beta 1 subunit	CCCAGACCACAGACTCTTAATTAG	TTAGAAATGACACCAGCCTCC
Atp11c	Mus musculus	ATPase, class VI, type 11C	CCAGCCCAGTTACCAGTG	CCTCACTCGCTTTGCATTTTC
Cdc42	Mus musculus	cell division cycle 42	CATGTCTCCTGATATCCTACACAAC	TGTCATAATCCTCTTGCCCTG
Anln	Mus musculus	anillin, actin binding protein	GGTTCCACTGAAAGCGAAATG	CTCATCGTCCACACTCATCTC
Birc5	Mus musculus	baculoviral IAP repeat-containing 5	AAGGAATTGGAAGGCTGGG	TTCTTGACAGTGAGGAAGGC
Ccna2	Mus musculus	cyclin A2	GTCCTTGCTTTTGACTTGGC	ACGGGTCAGCATCTATCAAAC
Ccnb1	Mus musculus	cyclin B1	CTGACCCAAACCTCTGTAGTG	CCTGTATTAGCCAGTCAATGAGG
Ccne2	Mus musculus	cyclin E2	GACGTTCATCCAGATAGCTCAG	TCCCATTCCAAACCTGAAGC
Grina	Mus musculus	glutamate receptor, ionotropic, N-methyl D-aspartate-associated protein 1	ATCTCCCTCATTGTTCTCAGC	ATGACTGCCTCCGTGTTG
Gabbr1	Mus musculus	gamma-aminobutyric acid (GABA) B receptor, 1	CCACACTCCACAATCCCAC	ATCTCAATCCCAGCCTCTTTC
Rbl1	Mus musculus	retinoblastoma-like 1 (p107)	AGAGTCAAGGAAGTTCGCAC	GGTCATCTCCAAACAGTCTCC
Rrm2	Mus musculus	ribonucleotide reductase M2	AAGCTCTGAAACCCGATGAG	TGGAAGCCATAGAAACAGCG
Cycs	Mus musculus	cytochrome c, somatic	AAGGGAGGCAAGCATAAGAC	ATTCTCCAAATACTCCATCAGGG
Dpp4	Mus musculus	dipeptidylpeptidase 4	AGTGCCTTAGTTGTGACCTG	TCGCAGCTCTTTATGATCCG
Ogt	Mus musculus	O-linked N-acetylglucosamine (GlcNAc) transferase	ATGGGAATCTCTGCTTGGATAAG	GCATAAGGTGTGAAGTAGGGTG
Tlr4	Mus musculus	toll-like receptor 4	TTCAGAACTTCAGTGGCTGG	TGTTAGTCCAGAGAAACTTCCTG
Tlr2	Mus musculus	toll-like receptor 2	ACAACTTACCGAAACCTCAGAC	ACCCCAGAAGCATCACATG
Tlr6	Mus musculus	toll-like receptor 6	CCGTCAGTGCTGGAAATAGAG	ACGATGGGTTTTCTGTCTTGG
Il7r	Mus musculus	interleukin 7 receptor	TCTGGAGAAAGTGGAAATGCC	AGCTGTGTTGATGTCTGAGTC
Cd19	Mus musculus	CD19 antigen	GAGAAGGAAAAGGAAGCGAATG	AGAGGTAGATGTAGGAAGGGAG
Fgf13	Mus musculus	fibroblast growth factor 13	AAAGACGAGGACAGCACTTAC	AGGTGTGAAATGTTCCGAGG
Lpar1	Mus musculus	lysophosphatidic acid receptor 1	CTATGTTCGCCAGAGGACTATG	GCAATAACAAGACCAATCCCG
Epb4.2	Mus musculus	erythrocyte membrane protein band 4.2	CACTATCACCCTGAACTTCCG	AGAGGAAATTGGGAAGATGGC
Epb4.9	Mus musculus	dematin actin binding protein	GAAAAGTCATTGCCCATCCG	AATTCTGTGGACTGTAGCCG

Rhd	Mus musculus	Rh blood group, D antigen	CGTGCGGCCAAGTATTTTG	GCAGACAAAAGGGACACAAAG
Rhag	Mus musculus	Rhesus blood group-associated A glycoprotein	TGGAGGTTTGCTTACAGGTC	ACGTGGTTGTGATTTGCATG
Spna1	Mus musculus	spectrin alpha, erythrocytic 1	CCTTAAATGTCCCCTCCAGTC	GTTCTTGATCTGCCTAGCCTC
Klf1	Mus musculus	Kruppel-like factor 1 (erythroid)	CCTCCATCAGTACACTCACC	CCTCCGATTTCAGACTCACG
Tac4	Mus musculus	tachykinin 4	AGAGGAACTGGCTTTTGGTG	GCTTCCCCATCAGACCATAG
Aqp1	Mus musculus	aquaporin 1	CTGGCGATTGACTACACTGG	AAGTCATAGATGAGCACTGCC
Snca	Mus musculus	synuclein, alpha	GGCAGTGAGGCTTATGAAATG	TGGAACTGAGCACTTGTACG
Cd36	Mus musculus	CD36 antigen	GCGACATGATTAATGGCACAG	GATCCGAACACAGCGTAGATAG
Nlrc4	Mus musculus	NLR family, CARD domain containing 4	GGAAAAGGATGGGAATGAAGC	CATCAATGTAGTGAGCTCTCCC
Epha7	Mus musculus	Eph receptor A7	AGAAGGAGAGTGGCTAGTACC	GGACAACGAGAACACTGGAG
Lpar1	Mus musculus	lysophosphatidic acid receptor 1	CTATGTTCGCCAGAGGACTATG	GCAATAACAAGACCAATCCCG
Met	Mus musculus	met proto-oncogene	GACCTCAGTGCTCTAAATCCAG	TCCAGCAAAGTCCCATGATAG
Hdc	Mus musculus	histidine decarboxylase	CGTTGCCTACACCTCTGATC	CCCTGTTGCTTGTCTTCCTC
Il6	Mus musculus	interleukin 6	AAACCGCTATGAAGTTCCTCTC	GTGGTATCCTCTGTGAAGTCTC
Il7	Mus musculus	interleukin 7	CCTCCACTGATCCTTGTTCTG	TCGGGCAATTACTATCAGTTCC
Ifng	Mus musculus	interferon gamma	AGGAACTGGCAAAAGGATGG	CAGGTGTGATTCAATGACGC
CreER^{T2}	Mus musculus	CreER^{T2}	CTAGGATGCGTACCATCGTAC	GGCATCCAGTCCCATCGATA
iDTR	Mus musculus	Inducible diphtheria toxin receptor	TACGCCTACCGCATCCGATCG	TGGAACCTCCGATTCCTAGC
S100a8	Mus musculus	S100 calcium binding protein A8 (calgranulin A)	AGTGTCCTCAGTTTGTGCAG	ACTCCTTGTGGCTGTCTTTG
S100a9	Mus musculus	S100 calcium binding protein A9 (calgranulin B)	GTTGATCTTTGCCTGTCATGAG	AGCCATTCCCTTTAGACTTGG
Gapdh	Mus musculus	glyceraldehyde-3-phosphate dehydrogenase	CTTTGTCAAGCTCATTTCCTGG	TCTTGCTCAGTGTCCTTGC

Table S1. Primers for quantitative RT-PCR, Related to Figure 1-3, S1-S6